Structural origin of set-reset processes in $Ge_{15}Te_{83}Si_2$ glass investigated using *in situ* Raman scattering and transmission electron microscopy

M. Anbarasu,[1] S. Asokan,[1,a)] Sudakshina Prusty,[2,b)] and A. K. Sood[2]
[1]*Department of Instrumentation, Indian Institute of Science, Bangalore 560012, India*
[2]*Department of Physics, Indian Institute of Science, Bangalore 560012, India*

(Received 22 January 2009; accepted 3 March 2009; published online 28 April 2009)

We report here that the structural origin of an easily reversible $Ge_{15}Te_{83}Si_2$ glass can be a promising candidate for phase change random access memories. *In situ* Raman scattering studies on $Ge_{15}Te_{83}Si_2$ sample, undertaken during the amorphous set and reset processes, indicate that the degree of disorder in the glass is reduced from off to set state. It is also found that the local structure of the sample under reset condition is similar to that in the amorphous off state. Electron microscopic studies on switched samples indicate the formation of nanometric sized particles of *c*-$SiTe_2$ structure. © *2009 American Institute of Physics*. [DOI: 10.1063/1.3115474]

I. INTRODUCTION

Phase change materials are one of the most promising materials for data storage applications. They are already successfully employed in optical data storage and offer great potential as an emerging nonvolatile electronic memory.[1–3] The main advantages of phase change memories (PCMs) are the large scaling capability, low voltages of operation, high data retention, direct write/overwrite capability, easiness to integrate with logic, etc.[4,5]

The basic operation of a PCM is based on a change in electronic/optical properties that occurs when the material transforms from a crystalline to an amorphous phase in a stable fashion under the excitation of electrical/optical stimulus.[1] The appreciable voltage-pulse-induced change in electrical resistance accompanying rapid and reversible phase transformations between crystalline and amorphous states in certain tellurides such as $(GeTe)_x(Sb_2Te_3)_y$, Ag–In–Sb–Te alloys,[3,6] etc., have been exploited so far for memory applications.

Despite a long history of memory switching in chalcogenide materials, understanding the physics of set (after memory switching)-reset (reamorphized) processes and optimization of the input electrical pulses such as amplitude, source resistance, pulse width, etc., still remain incomplete. Usually, a higher current is required for resetting the memory state, and reduction in reset current is one of the most crucial aspects for developing high-density (lower programming volume) phase change random access memories (PCRAMs).[4–8] Many attempts have been made to reduce the reset current by modifying the device structure or by doping with other elements to reduce the melting temperature and eventually to reduce the programming volume.[9]

In the present work, a new phase change material ($Ge_{15}Te_{83}Si_2$) is identified, which is relatively easily devitrifiable, and at the same time having a better glass formability.[10] Though the electrical switching process in $Ge_{15}Te_{83}Si_2$ glass may be slower compared with $Ge_2Te_5Sb_2$ due to its low quenching rate,[7–9] the sample has other advantages such as larger difference in resistance between the on and off states, good thermal stability, etc., and is likely to be a suitable material for PCRAM applications.[10–12] It is therefore important to understand the structural properties, local structural changes during set and reset operations, etc., of the $Ge_{15}Te_{83}Si_2$ glass.

This paper deals with the *in situ* Raman scattering experiments performed on $Ge_{15}Te_{83}Si_2$ sample, during the electrical set-reset processes, in order to elucidate the local structural changes during the set and reset operations. X-ray diffraction (XRD) and transmission electron microscopic (TEM) studies have also been carried out on amorphous, switched, and thermally annealed samples to probe the structural transformations during the set and reset processes.

II. EXPERIMENTAL DETAILS

Bulk $Ge_{15}Te_{83}Si_2$ glass has been prepared by vacuum-sealed melt quenching method. Appropriate quantities of high purity (99.95%) constituent elements are sealed in an

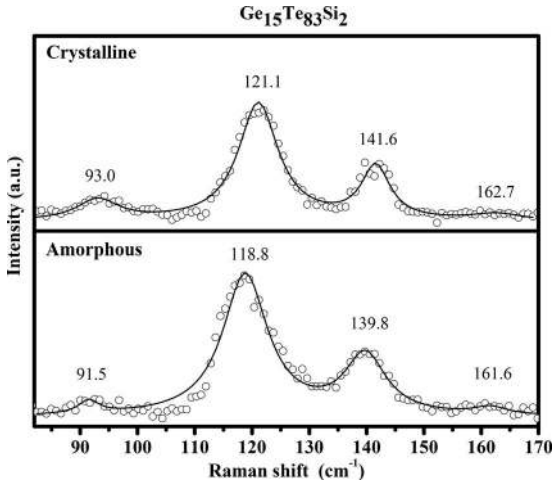

FIG. 1. Comparison between the Raman spectra of amorphous and crystalline $Ge_{15}Te_{83}Si_2$.

a)Electronic mail: sasokan@isu.iisc.ernet.in.
b)Present address: Visiting Faculty, School of Physics, National Institute of Science Education and Research, Bhubaneswar 751005, India.

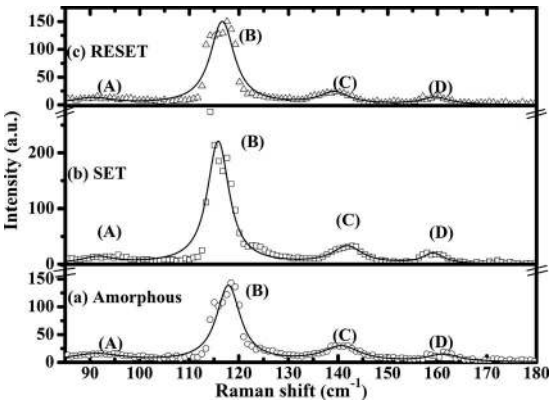

FIG. 2. *In situ* Raman scattering studies on (a) amorphous sample, (b) electrically switched (set), and (c) reamorphized (reset) states.

evacuated (at 10^{-6} mbar) quartz ampoule and are slowly heated at the rate of 100 °C/h until 1100 °C in a horizontal rotary furnace. The ampoules are maintained at 1100 °C and rotated continuously for about 24 h at 10 rpm to ensure homogeneity of the melt. The ampoules are subsequently quenched in a bath of ice water and NaOH mixture to get bulk glassy samples. The amorphous nature of the as-quenched sample is confirmed by XRD (Philips powder diffractometer; Cu $K\alpha_1$, $\lambda = 1.5405$ Å) method.

A gap-cell arrangement, with a channel width of ~0.3 mm and with gold coated electrodes, has been used for *in situ* Raman scattering studies during electrical switching on $Ge_{15}Te_{83}Si_2$ samples of dimensions approximately $3 \times 3 \times 0.4$ mm^3. The external connections have been made with copper wires using silver paste.

The confocal micro-Raman studies have been carried out in backscattering geometry using DILOR-XY instrument equipped with a liquid nitrogen-cooled charge coupled device (CCD) detector. The samples have been illuminated by the 514.5 nm line of an argon ion laser (COHERENT INNOVA 300) focused at a spot of glassy sample in between the gold electrodes. All the data are recorded using ~2 mW of laser power (which does not affect the local structure) and for about 600 s of accumulation. The spectral resolution is 0.8 cm^{-1}. The Raman spectra have been acquired in three different stages, namely, as-quenched, set, and reset states.

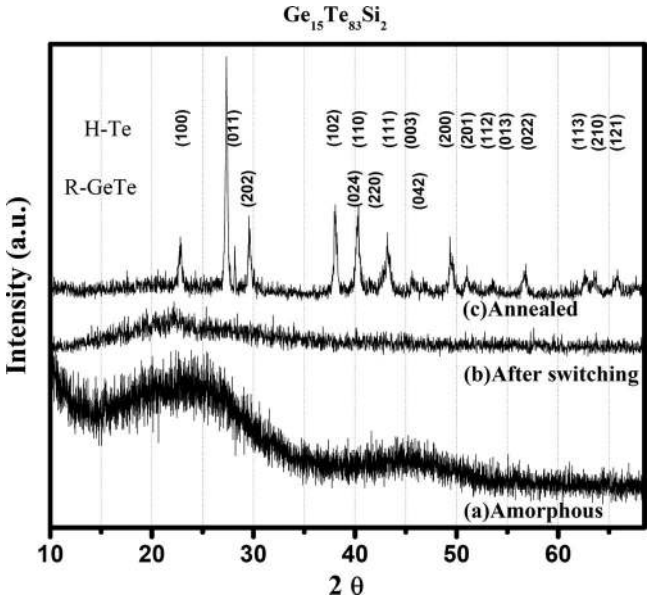

FIG. 3. XRD patterns of $Ge_{15}Te_{83}Si_2$ sample (a) as-quenched, (b) after switching, and (c) after annealing at 350 °C for 2 h.

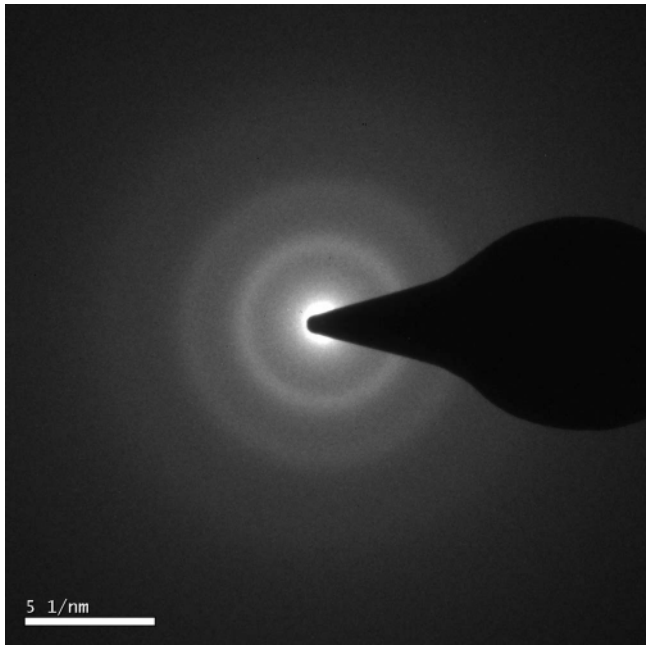

FIG. 4. TEM image of $Ge_{15}Te_{83}Si_2$ glass.

TABLE I. Line shape fitting parameters of the Raman spectra of $Ge_{15}Te_{83}Si_2$ in amorphous, set, and reset conditions.

Sample No.	Peak	Line shape	Amorphous	Set	Reset
I	*A*	Position	91.7 ± 1.5	92.1 ± 2.7	91 ± 1.9
		Linewidth	12.6 ± 5	7.3 ± 8.4	9.8 ± 6.5
II	*B*	Position	117.9 ± 0.1	115.8 ± 0.1	116.6 ± 0.1
		Linewidth	5.6 ± 0.3	5 ± 0.3	5.6 ± 0.3
III	*C*	Position	140.7 ± 0.6	141.8 ± 1	139.2 ± 0.8
		Linewidth	8.9 ± 1.8	7.1 ± 3.1	7.1 ± 2.5
IV	*D*	Position	161.2 ± 1.1	159.2 ± 1.4	159.6 ± 1.3
		Linewidth	7.2 ± 3.2	4.8 ± 4.2	6.4 ± 3.9

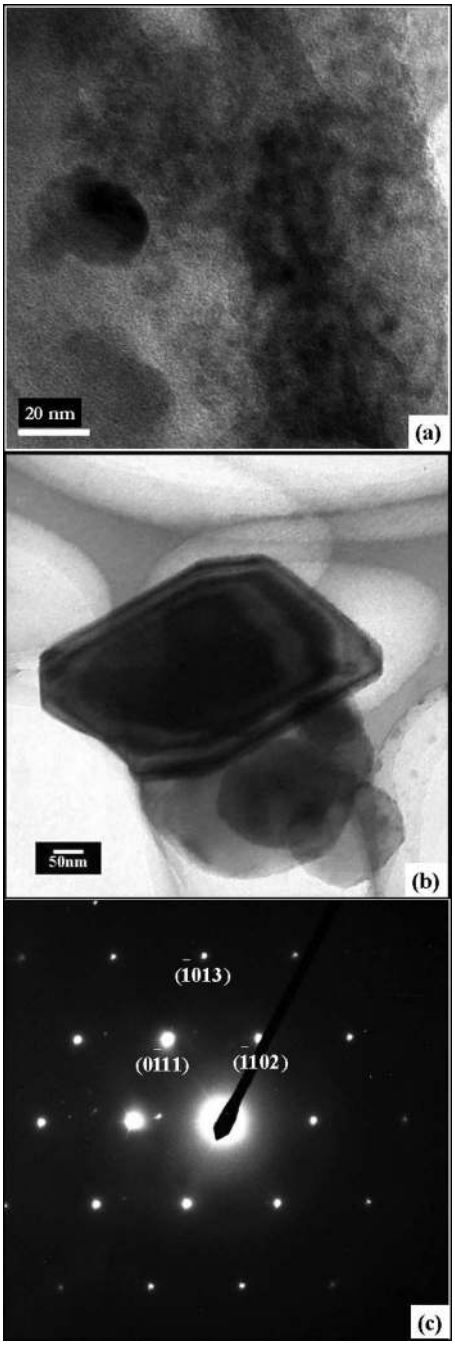

FIG. 5. BF of (a) switched sample in which the dark spots show the crystalline region, (b) faceted particles of the switched sample, and (c) electron diffraction pattern of the faceted particle.

The *in situ* electrical set-reset processes are performed on the surface of the sample whereas the remaining electrical measurements have been undertaken across the sample.[10] The sample behavior is found to be similar in both cases.

The preliminary structural analyses are carried out on switched samples using a JEOL 2000 FX II TEM (200 kV). To probe the structural details further, a FEI TECNAI high resolution transmission electron microscope (HRTEM) (300 kV) is used. Samples are prepared for the TEM experiments by spreading the powered samples on the grid, and they are found to be stable with the applied electric field.

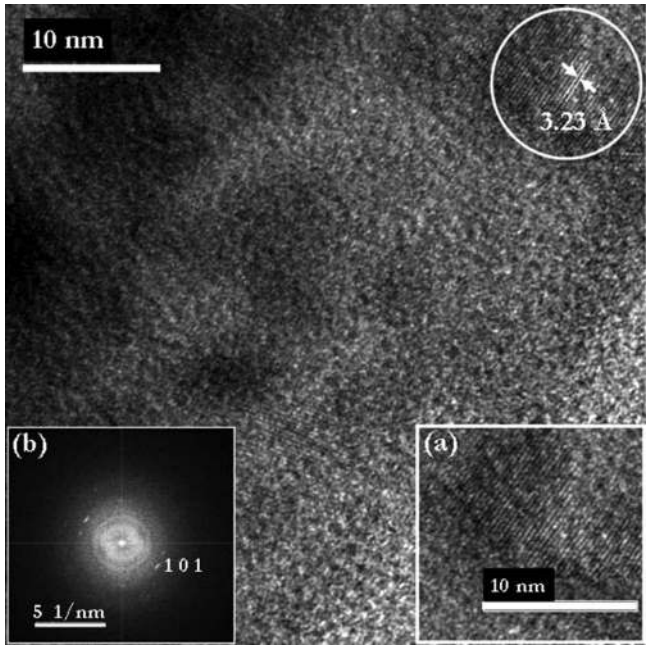

FIG. 6. HRTEM image of the switched samples indicating the crystalline fringes formed during the set process: (a) magnified region of the crystalline fringes and (b) FFT of the electron diffraction pattern.

III. RESULTS AND DISCUSSION

A. *In situ* Raman scattering studies during set and reset conditions

Figure 1 shows a comparison between the Raman spectra of a bulk $Ge_{15}Te_{83}Si_2$ glass and the corresponding crystal obtained by thermal annealing well above the crystallization temperature. The Raman spectrum of the crystal shows an overall redshift as compared to the amorphous one.

Figure 2 shows the Raman spectra of $Ge_{15}Te_{83}Si_2$ glass obtained during various stages, namely, as-quenched, after the set and reset processes. Here, the Raman spectra have been recorded in three sequential stages. At first stage, the Raman spectrum of an amorphous sample is obtained by focusing at a spot in the chalcogenide glass in between the gold electrodes. In the second step, the spectrum has been acquired by focusing the laser beam at a spot in the conducting crystalline channel formed during the set process. In third step, the spectrum is obtained after resetting the conducting channel by passing a short width rectangular current pulse. The three different phases of sample, namely, amorphous, set, and reset states, have been confirmed by measuring the electrical resistance between electrodes (approximately 0.3 MΩ for amorphous, 56 Ω for set, and 0.3 MΩ for reset states, respectively).

It is seen in Fig. 2 that there are three main bands in the Raman spectra of the amorphous, set, and reset states, in the frequency range of 85–180 cm^{-1}. Approximate wave number ranges of the band positions for all the three states are as follows: band $B \sim 115.8–117.9$ cm^{-1}, band $C \sim 139.2–141.8$ cm^{-1}, band $D \sim 159.2–161.2$ cm^{-1}, and a weak hump band $A \sim 91.7–92.1$ cm^{-1}. The details of the line shape fitting parameters are given in Table I.

Figure 2(a) shows the Raman spectrum of the $Ge_{15}Te_{83}Si_2$ glass, which exhibits three distinct peaks around

117.9 (*B*), 140.7 (*C*), and 161.2 cm^{-1} (*D*), respectively. The spectrum also has a weak hump around 91.7 cm^{-1} (*A*). Peak *B* can be attributed to the A_1 mode and peaks *A* and *C* to the E_{TO} modes of crystalline Te–Te chain.[13]

In the present study, the composition of the base glass ($Ge_{15}Te_{85}$) is well below the critical composition, $Ge_{33}Te_{77}$, defined by the chemically ordered covalent network model. This model presumes that the Te atoms are arranged as one-dimensional chains, between which the Ge atoms are present as cross-links.[14] Thus, the structural network in the base glass is primarily decided by Te–Te chains, which are interlinked by Ge–Te bonds. It is also known that amorphous Te crystallizes at 10 °C and is unstable at room temperature.[15] Therefore, the Te-atom chains in $Ge_{15}Te_{83}Si_2$ glass are likely to have a certain degree of order. This conjecture is consistent with the observation that Raman peaks *A*–*C* in $Ge_{15}Te_{83}Si_2$ glass correspond to the modes of crystalline Te.

It is also interesting to note from Raman studies on Si–Te glasses[16] that there exists a peak at 138 cm^{-1}, attributed to the tetrahedral $SiTe_{4/2}$ units, and shows a blueshift toward 141 cm^{-1} during thermal annealing. Hence, the peak at 140.7 cm^{-1} (*C*) can be attributed to the Te chain as well as to the vibrational motions in $SiTe_{4/2}$ face-sharing tetrahedra. Further, peak *D* can be assigned to the symmetric stretching mode of the edge-sharing $GeTe_4$ tetrahedra.[14]

The Raman spectrum of the $Ge_{15}Te_{83}Si_2$ sample, acquired by focusing the beam on the switched region after the set process, is shown in Fig. 2(b). It is interesting to note that there are no drastic changes in the Raman spectra of the $Ge_{15}Te_{83}Si_2$ sample during the set transition: While peak *A* remains almost unaffected, peaks *C* and *D* exhibit marginal blue- and redshifts (about one wave number each), respectively. However, peak *B* at 117.9 cm^{-1} becomes more intense during the set operation.

It can be observed from the present *in situ* Raman studies that the local structure remains mostly unaltered during the set process, while the degree of disorder is reduced in the Te-atom chains present in the glass $Ge_{15}Te_{83}Si_2$ system keep-

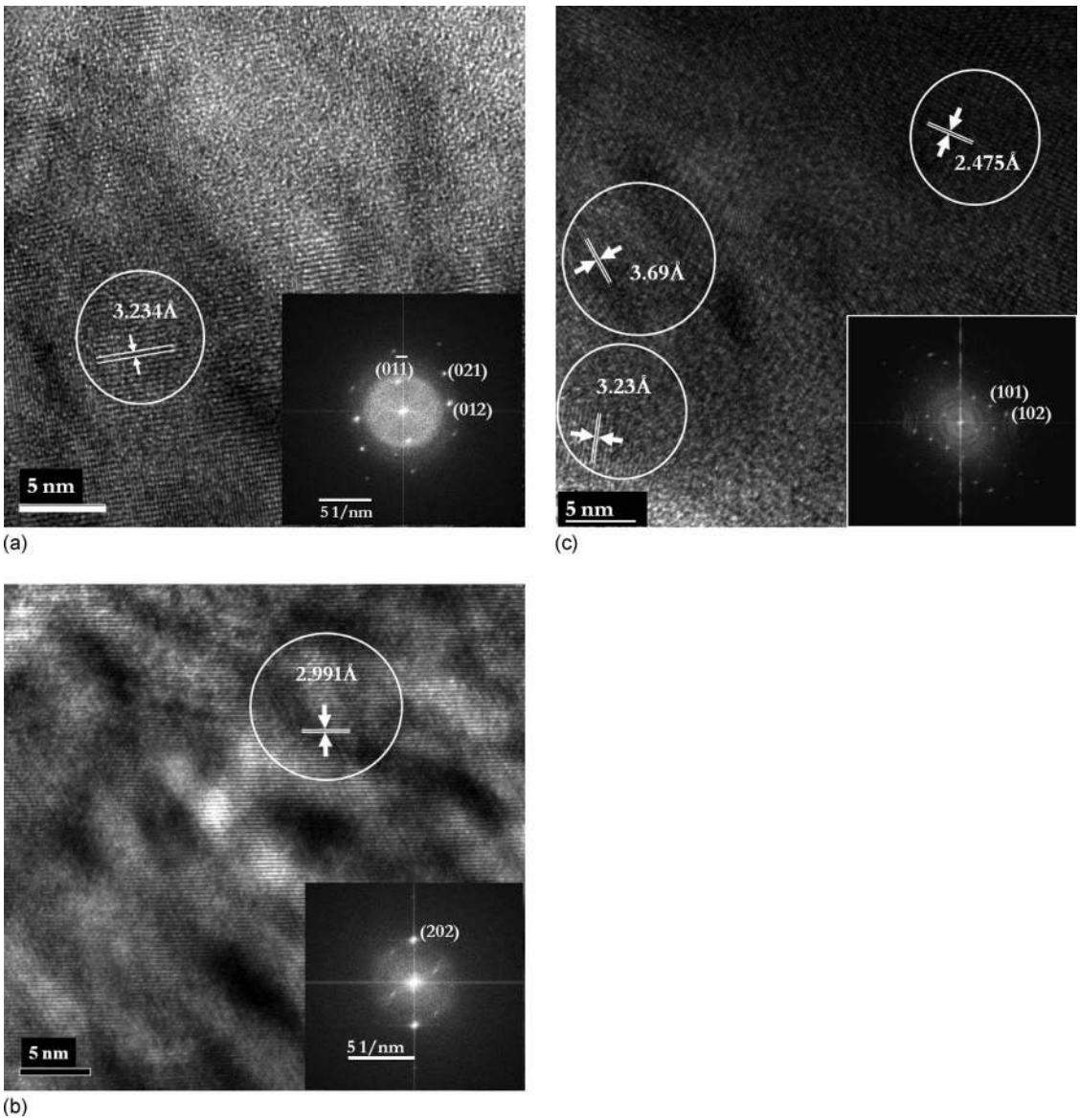

FIG. 7. (a) HRTEM images on thermally annealed samples indicating *c*-Te structure, and the inset shows the FFT of electron diffraction. (b) HRTEM images on thermally annealed samples indicating *c*-GeTe structure, and the inset shows the FFT of electron diffraction. (c) HRTEM images on thermally annealed samples indicating *c*-$SiTe_2$ structure, and the inset shows the FFT of electron diffraction.

ing the original glassy network intact. This behavior is in contrast to other GeTe systems.[14] In this case, there is no large scale amorphous-crystal phase transition during the set process. Rather, a much localized local structural rearrangement takes place in the sample, which causes a large change in the electrical properties.

Figure 2(c) shows the Raman spectrum of the $Ge_{15}Te_{83}Si_2$ sample, acquired by focusing the beam on the switched region after the reset process. It is clear from this figure that the Raman spectrum of the sample in the reset state is very similar to the amorphous spectrum. The present *in situ* Raman studies indicate that in the Ge–Te–Si sample, the local structures in the glassy (off state) and reset states are similar and they are not very different from the local structure in the set state. This implies that the three states are close to each other in terms of local structure, and the transitions between them are likely to be less energy intensive. These observations are consistent with the electrical switching results, which indicate that the Ge–Te–Si sample can be set with a relatively lower current (1 mA for a 0.15 mm thick sample) and it is electrically easily resettable with the same magnitude of current and also the sample gets self reset with a sawtooth current pulse.[10]

B. X-ray diffraction studies

The XRD pattern of the as-quenched $Ge_{15}Te_{83}Si_2$ sample is shown in Fig. 3(a), which indicates the amorphous nature of the sample. It is interesting to note that the diffraction pattern of the sample after switching also does not depict any sharp diffraction peaks [Fig. 3(b)]. The crystallization occurring in the sample during switching is local and restricted only to the electrode region, and therefore it does not show up in the XRD studies. The powder pattern of thermally annealed samples is shown in Fig. 3(c), which contains crystalline peaks corresponding to hexagonal *c*-Te (a=4.4572 Å and c=5.929 Å) and rhombohedral *c*-GeTe (a=8.3428 Å and c=10.668 Å).

C. Transmission electron microscopic studies

Figure 4 shows the TEM image of the as-quenched $Ge_{15}Te_{83}Si_2$ glass; the absence of diffraction contrast in the TEM image confirms the amorphous nature of the sample. The TEM images of the switched $Ge_{15}Te_{83}Si_2$ sample indicate the formation of nanometric sized crystals (as dark spherical particle) embedded in an amorphous matrix shown in Fig. 5(a). The bright field (BF) image and the $[5\bar{1}43]$ zone axis are shown in Figs. 5(b) and 5(c); the crystal structure has been identified as hexagonal *c*-$SiTe_2$ (with a space group of $P3m1$; a=4.28 Å and c=6.70 Å).

HRTEM analysis has been performed on switched samples in order to further confirm the crystal structure (Fig. 6). The HRTEM image reveals crystalline fringes formed during the set operation corresponding to hexagonal *c*-$SiTe_2$ structure, which is embedded in the amorphous matrix.

In addition, HRTEM analysis has been undertaken on thermally annealed $Ge_{15}Te_{83}Si_2$ samples, which reveals the presence of hexagonal Te (a=4.4572 Å and c=5.929 Å), rhombohedral GeTe (a=8.3428 Å and c=10.668 Å), and hexagonal $SiTe_2$ (a=4.28 Å and c=6.70 Å). Figures 7(a)–7(c) show the lattice fringes of the Te, GeTe, and $SiTe_2$ crystals and the corresponding fast Fourier transform (FFT) as inset, respectively. It can be noticed that the HRTEM analysis on thermally annealed samples is in good agreement with the XRD results obtained.

IV. CONCLUSIONS

In situ Raman scattering studies on $Ge_{15}Te_{83}Si_2$ sample, undertaken during the set and reset processes, indicate that the degree of disorder in the glass is reduced from off to set state. It is found that the changes in the Raman spectra during the set operation are peaks *C* and *D* exhibit marginal blue- and redshifts corresponding to face-sharing $SiTe_{4/2}$ tetrahedra and edge-sharing $GeTe_4$ tetrahedra, respectively, and also peak *B* becomes more intense. It is also found that the local structure of the sample under the reset condition is similar to that in the amorphous state. Electron microscopic studies on switched samples indicate that the formation of nanometric sized particles of *c*-$SiTe_2$ structure is a possible crystalline structure formed during the set operation, which also likely to be supportive with the Raman studies.

ACKNOWLEDGMENTS

A.K.S. thanks the Department of Science and Technology for financial support. The financial support of Applied Materials Inc. is also gratefully acknowledged. The fruitful discussions with Dr. K. K. Singh, Applied Materials Inc., are highly appreciated.

[1] M. Wuttig, Nature Mater. **4**, 265 (2005).
[2] M. H. R. Lankhorst, B. W. M. M. Ketelaars, and R. A. M. Wolters, Nature Mater. **4**, 347 (2005).
[3] M. Wuttig and N. Yamada, Nature Mater. **6**, 824 (2007).
[4] S. Hudgens and B. Johnson, MRS Bull. **29**, 1 (2004).
[5] D.-H. Kang, B.-k. Cheong, J.-h. Jeong, T. S. Lee, I. H. Kim, W. M. Kim, and J-Y. Huh, Appl. Phys. Lett. **87**, 253504 (2005).
[6] W. Welnic and M. Wuttig, Mater. Today **11**, 20 (2008).
[7] A. Pirovano, A. L. Lacaita, A. Benvenuti, F. Pellizzer, and R. Bez, IEEE Trans. Electron Devices **51**, 452 (2004).
[8] A. Redaelli, A. Pirovano, F. Pellizzer, A. L. Lacaita, D. Lemini, and R. Bez, IEEE Electron Device Lett. **25**, 684 (2004).
[9] B. Qiao, J. Feng, Y. Lai, Y. Ling, Y. Lin, T. Tang, B. Cai, and B. Chen, Appl. Surf. Sci. **252**, 8404 (2006).
[10] M. Anbarasu, S. Asokan, S. Prusty, and A. K. Sood, Appl. Phys. Lett. **91**, 093520 (2007).
[11] M. Anbarasu and S. Asokan, J. Phys. D: Appl. Phys. **40**, 7515 (2007).
[12] M. Anbarasu, K. K. Singh, and S. Asokan, Philos. Mag. **88**, 599 (2008).
[13] A. S. Pine and G. Dresselhaus, Phys. Rev. B **4**, 356 (1971).
[14] K. S. Andrikopoulos, S. N. Yannapoulos, G. A. Voyiatzis, A. V. Kolobov, R. Ribes, and J. Tominaga, J. Phys.: Condens. Matter **18**, 965 (2006).
[15] M. H. Brodsky, R. J. Gambino, J. E. Smith, and Y. Yacoby, Phys. Status Solidi B **52**, 609 (1972).
[16] B. Norban, D. Pershing, R. N. Enzweiler, P. Boolchand, J. E. Griffiths, and J. C. Phillips, Phys. Rev. B **36**, 8109 (1987).